Journal of Power Sources 196 (2011) 6982–6986

Contents lists available at ScienceDirect

Journal of Power Sources

journal homepage: www.elsevier.com/locate/jpowsour

Short communication

High performance Si/C@CNF composite anode for solid-polymer lithium-ion batteries

Q. Si, K. Hanai, T. Ichikawa, A. Hirano, N. Imanishi, O. Yamamoto, Y. Takeda*

Department of Chemistry for Materials, Graduate School of Engineering, Mie University, 1577 Kurimamachiya-cho, Tsu, Mie 514-8507, Japan

ARTICLE INFO

Article history:
Received 11 August 2010
Received in revised form 14 October 2010
Accepted 25 October 2010
Available online 2 November 2010

Keywords:
PEO-based electrolyte
Lithium-ion battery
Si/C@CNF composite
Irreversible capacity
Safety

ABSTRACT

The electrochemical performance of a composite of nano-Si powder and a pyrolytic carbon of polyvinyl chloride (PVC) with carbon nanofiber (CNF) was examined as an anode for solid-polymer lithium-ion batteries. Nano-Si powder was firstly coated with carbon by pyrolysis of PVC and then mixed with CNF (referred to as Si/C@CNF) using a rotation mixer. The composite exhibited good cycling performance, but suffered from a large irreversible capacity loss of which the retention was less than 60%. In order to reduce the loss, a thin lithium sheet was attached to the Si/C@CNF electrode surface as a reducing agent. The irreversible capacity of the first cycle was lowered to as much as 0 mAh g^{-1} and after the third cycle, the lithium insertion and extraction efficiency was almost 100%. A reversible capacity of more than 1000 mAh g^{-1} was still maintained after 40 cycles.

1. Introduction

Lithium-ion batteries are one of the great successes from the application of advanced materials and electrochemistry to modern energy storage devices. The energy density for small size batteries of this type is as high as 200 Wh kg^{-1}. In recent years, higher energy density batteries of larger size have been required for applications such as hybrid electric vehicles (HEVs), electric vehicles (EVs) and load leveling devices. However, a battery device with higher energy density also includes a higher risk of fire or explosion. From this point, safety performance is an important issue for applications of lithium-ion batteries. An all-solid state battery that employs a nonflammable solid polymer electrolyte (SPE) may be a reasonable solution to address these safety issues.

Solid-polymer lithium-ion batteries, which have mainly used a lithium metal anode and oxide cathode [1] have been extensively studied for several decades. Although lithium metal anode contributes to a high energy density, it has safety problems arising from dendrite formation on the anode surface [2]. Graphite anodes have exhibited excellent electrochemical performance and good safety performance in ethylene carbonate based electrolyte. Therefore, graphite and related carbon materials have been widely used as the anode in lithium-ion batteries, and the study of graphite in solid-polymer electrolyte has been intensively investigated in recent years. We have previously reported the improved reversibility of a graphite anode with a polymer electrolyte by surface modification of the graphite [3]. This approach enabled the active control of the solid electrolyte interface (SEI) from the graphite surface.

On the other hand, silicon is a most promising material for such applications, due to its high theoretical capacity (4200 mAh g^{-1}) [4]. However, large volume changes occur in Si during Li-insertion and extraction, which causes pulverization of the active materials followed by a loss of electrical contact. As a result, the Si electrode shows a rapid capacity fade [5,6]. One of the most promising methods to solve this problem is to disperse Si into a carbon matrix [7–9], in which the carbon phase acts as both a structural buffer and an electrochemically active material. Other silicon-based anode materials have been synthesized and investigated [10–14]. Liu et al. reported that the combination of a SiO/$Li_{2.6}Co_{0.4}N$ composite electrode in solid poly(ethylene oxide) (PEO) electrolyte resulted in a high first cycle efficiency of ca. 100%; however, the reversible capacity was low as ca. 500 mAh g^{-1} [10]. Kobayashi et al. [11] reported the combination of graphite or SiO/graphite with a SPE. The reversible capacities were 360 mAh g^{-1} for graphite and 1000 mAh g^{-1} for SiO/graphite and the retention was 75% at the 250th cycle versus the initial capacity for graphite, and 72% at the 100th cycle for SiO/graphite. However, the SiO/graphite electrode shows a lower first cycle efficiency with a SPE.

We have previously reported the excellent cycling performance of an amorphous carbon-coated Si anode with carbon nanofiber (CNF) (referred to as Si/C@CNF) in liquid electrolyte [15]. However, the composite has high irreversible capacity in the first cycle. In this study, we focus our attention on the electrochemical behavior of lithium insertion into and extraction from the Si/C@CNF composite

* Corresponding author. Tel.: +81 59 231 9419; fax: +81 59 231 9478.
E-mail address: takeda@chem.mie-u.ac.jp (Y. Takeda).

0378-7753/$ – see front matter © 2010 Elsevier B.V. All rights reserved.
doi:10.1016/j.jpowsour.2010.10.091

electrode in PEO-based electrolytes. We have introduced a certain amount of lithium metal sheet into the Si/C@CNF electrode in an attempt to compensate the first irreversible capacity that results in a high initial coulombic efficiency (referred to as a "precharged electrode").

2. Experimental

Nano-Si powder (particle size 50 nm, purity >98%) and polyvinyl chloride (PVC) were purchased from Aldrich. CNF (diameter: 10–20 nm, length: 0.1–10 μm) was purchased from Jemco, Japan. The nano-Si/carbon composite (Si/C) was prepared according to the previously reported method [7]. Si particles are surrounded by and embedded in the amorphous porous carbon formed by the thermal decomposition of PVC. The Si/C weight ratio was confirmed to be almost 1:1 from chemical analysis. The Si/C@CNF electrode material was prepared according to the previously reported method [15]. The Si/C composite was mixed with CNF (Si/C:CNF = 3:1 in weight) in 1-methyl-2-pyrrolidone (NMP) solution using a rotation mixer. The working electrode was prepared from a mixture of the active materials and poly (vinylidene fluoride) (PVDF) with a Si/C@CNF:PVDF ratio of 80:20 by weight. The mixtures of the electrode components in NMP were uniformly painted onto copper foils, and dried at 80 °C for 1 h. The painted electrodes were cut to a size of $1 \times 1\ cm^2$ and further dried at 120 °C under vacuum for 2 h, followed by pressing at 200 kgf cm^{-2}. The precharged electrode was prepared by attaching a thin lithium sheet onto the rim of the Si/C@CNF electrode surface. The specific capacity was based on the weight of Si/C.

The PEO-based polymer electrolyte was prepared as follows: PEO (Aldrich, average molecular weight: 6×10^5) and $Li(CF_3SO_2)_2N$ (LITFSI, Fluka) were dissolved in acetonitrile (AN) with Li/O at a molar ratio of 1/18. The polymer electrolyte solution was cast into a polytetrafluoroethylene (PTFE) dish under an Ar atmosphere. After evaporation of the AN at room temperature, the formed film was dried at 110 °C for 12 h under vacuum. Prior to construction of the laminate cell, the combined active material and PEO sheet were preheated at 80 °C for 3 h and then charged and discharged at 60 °C in the voltage range of 0.02–1.5 V using a Nagano BTS 2004H battery cycler. The resulting film thickness was approximately 300 μm. The entire system, Cu/active material/PEO sheet/Li/Cu, was then sealed into a laminate cell for electrochemical testing. The charge and discharge rates were typically set at C/10. The morphology of the electrode was examined using scanning electron microscopy (SEM; Hitachi S-4800). Cyclic voltammograms (CVs) were measured using an automatic polarization system (Hokuto Denko HSV-110). Differential scanning calorimetry (DSC; Rigaku Thermo Plus 8330) measurements were conducted using samples of electrode and electrolyte mixtures packed and sealed in a stainless steel pan under an Ar atmosphere at a scanning rate of 3 °C min^{-1} and with Al_2O_3 as a reference.

3. Results and discussion

To suppress instability of the electrode morphology upon Li insertion and extraction, nano-Si can be dispersed within an inert matrix containing pyrolytic carbon and CNF. Fig. 1 shows SEM images of CNF (Fig. 1a) and the Si/C@CNF composite (Fig. 1b). Si/C mixed with CNF in NMP is uniformly dispersed in the tangled CNF net. The Si/C@CNF composite electrode was approximately 60–70 μm thick with the active material loaded at 0.5–0.7 mg cm^{-2}. The charge–discharge characteristics of the Si/C@CNF anodes with a liquid electrolyte of 1 M $LiClO_4$ in ethylene carbonate and diethylene carbonate (EC/DEC, 1:1 vol%) and the PEO-based electrolyte as a solid electrolyte are shown in Fig. 2. The operation temperature

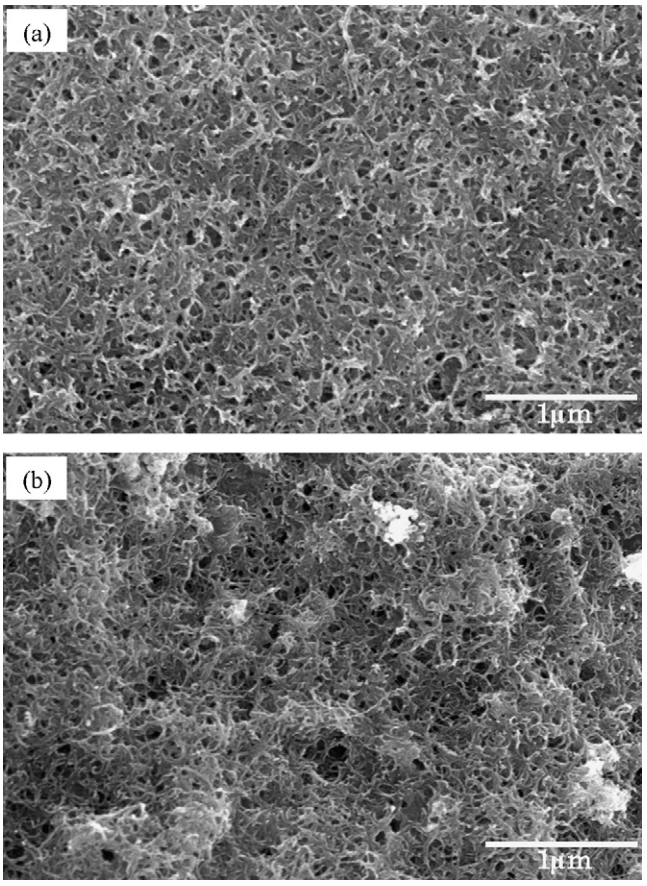

Fig. 1. SEM images of (a) CNF and (b) the Si/C@CNF composite.

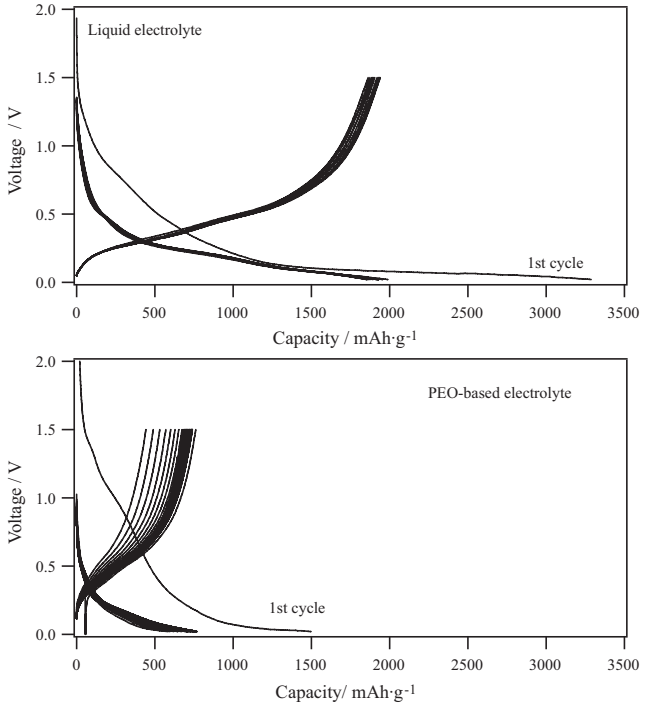

Fig. 2. Charge–discharge curves of the Si/C@CNF composite electrode with a liquid electrolyte (EC-DEC-$LiClO_4$) at room temperature and with the PEO-based electrolyte (PEO-$Li(CF_3SO_2)_2N$) at 60 °C.

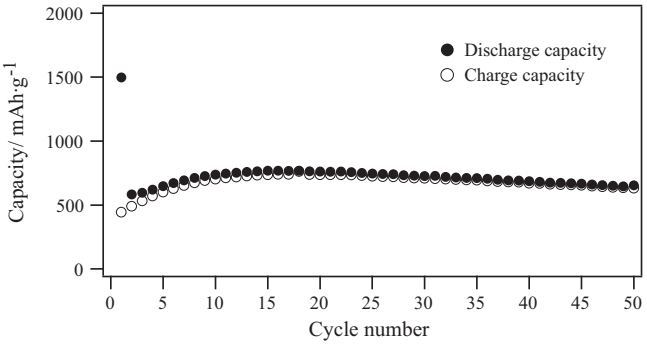

Fig. 3. Cycling performance of the Si/C@CNF electrode with the PEO-based electrolyte at 60 °C. The thickness of the Si/C@CNF electrode was ca. 70 μm.

was fixed at room temperature for the liquid electrolyte cells and at 60 °C for the PEO-based electrolyte cells. Although the temperatures for these cells were different, they provide a baseline for practical application of such cells under appropriate conditions for the respective electrolytes to exhibit sufficient conductivity.

The Si/C@CNF electrode shows a high reversible capacity of ca. 2000 mAh g^{-1} in the liquid electrolyte from the second cycle. In contrast, the cell with PEO-based electrolyte exhibits a smaller capacity of ca. 500 mAh g^{-1}. However, the cycling performance of the PEO-based electrolyte cell in Fig. 3 shows an increase in capacity with the cycle number with a cycling efficiency of almost 97%. The lower capacity of the PEO based cell compared with the liquid electrolyte cell is explained by the small active contact area between the electrode and electrolyte. The Si/C@CNF electrode in this study contains no PEO-based electrolyte. Typically, the electrolyte is also mixed with the active electrode materials for the preparation of an all-solid state cell. We prepared electrodes with various combinations of the PEO electrolyte and active materials; however, no suitable performance was obtained. Therefore, in order to reduce the lithium diffusion length, a thinner electrode was prepared and the performance was examined. Heat treatment of the electrode/PEO electrolyte system was also performed at 80 °C with the expectation that the PEO electrolyte would infiltrate into the electrode. The electrochemical performance of heat-treated (80 °C) anode with the PEO-based electrolyte at 60 °C is shown in Fig. 4, where the thickness of the Si/C@CNF electrode was approximately 30 μm, and the loaded active material was 0.2 mg cm^{-2}. The reversible capacity was enhanced to 2151 mAh g^{-1} in the second cycle, which is almost comparable to that for the liquid electrolyte system. This result implies that even in a polymer electrolyte system, an increase of the contact area between the active material and the electrolyte can increase the utilization of the active material. The graphite anode for the solid polymer lithium battery also exhibited similar behavior [3,16]. Unfortunately, the capacity fade is much larger than that for the liquid electrolyte, and this will be discussed later.

Another problem for the Si/C@CNF electrode with the PEO-based electrolyte cell is the low initial coulombic efficiency, which was as low as 44%. The Si/C@CNF electrode also showed a low initial coulombic efficiency of 58% in the liquid electrolyte. This can be attributed to irreversible Li–Si alloy formation, the electrochemical reduction of electrolyte on the anode surface, and the large irreversible capacity of CNF itself.

Jarvis et al. reported a pre-lithiation method using lithium metal powder to reduce the first irreversible capacity [17]. In the present study, a precharged electrode was realized by placing a thin lithium sheet onto the Si/C@CNF electrode surface. As shown in Fig. 4, the irreversible capacity of the original electrode in the 1st cycle was approximately 2490 mAh g^{-1}. The weight of the active material in the original electrode was 0.2 mg; therefore, the irreversible capacity was approximately 0.498 mAh. The weight of lithium metal was calculated on the basis of the amount of irreversible capacity and was approximately 0.13 mg. The actual amount of lithium added was approximately 0.15 mg.

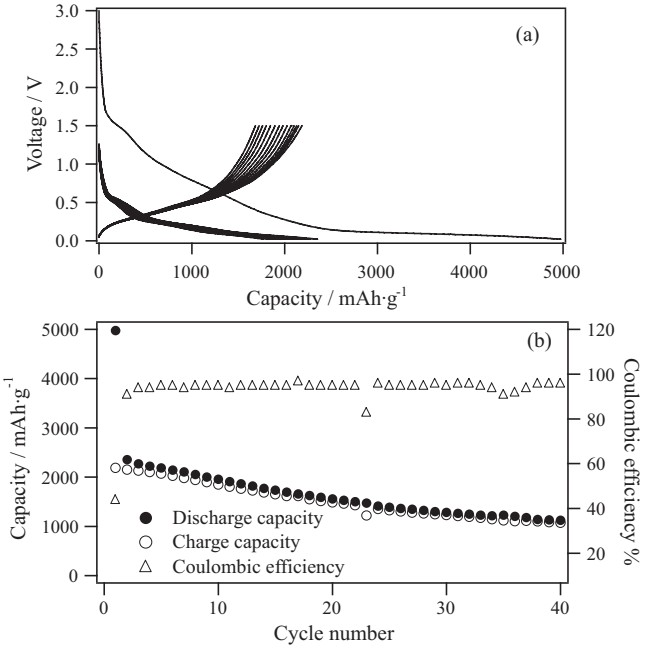

Fig. 4. (a) Charge and discharge curves and (b) cycling performance of the Si/C@CNF thin electrode with the PEO-based electrolyte at 60 °C. The thickness of the Si/C@CNF electrode was ca. 30 μm.

Fig. 5 shows cyclic voltammograms for the original and precharged electrodes with the PEO-based electrolyte for the first cycle measured between 0 and 2.5 V at a scan rate of 0.017 mV s^{-1}. Three current peaks appear for the non-precharged electrode (original electrode) at potentials of 1.4, 1.0, and 0 V in the first reduction half-cycle (lithium insertion). The potentials of the two former peaks may correspond to (1) the reductive decomposition of the electrolyte and the subsequent formation of the SEI film on the surface of the active particles and (2) lithium insertion into the CNF structure, from which the lithium ions are not extracted in the following charge process. In the CV profile of the precharged electrode, only a peak at around 0.5–0 V was observed in the first reduction sweep, which indicates the formation of Li–Si alloys. Side reactions observed in the original electrode are already completed prior to

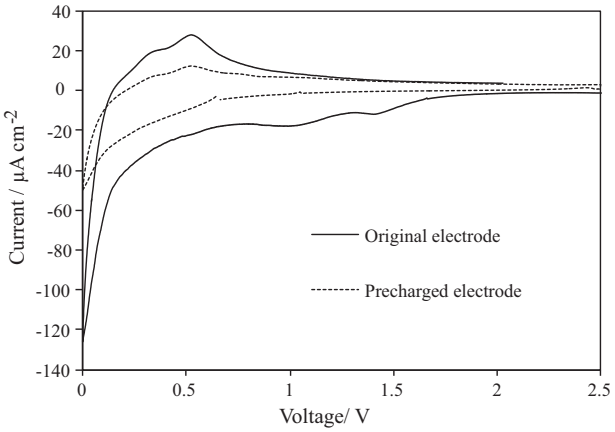

Fig. 5. Cyclic voltammograms (CVs) of the original and precharged electrodes with PEO-based electrolyte for the first cycle. The voltage was scanned in the range of 0–2.5 V at a scan rate of 0.017 mV s^{-1}.

Table 1
Cycle performance of the original and precharged electrodes.

Cycle number	Original electrode			Precharged electrode		
	Charge capacity ($mAh\,g^{-1}$)	Discharge capacity ($mAh\,g^{-1}$)	Coulombic efficiency (%)	Charge capacity ($mAh\,g^{-1}$)	Discharge capacity ($mAh\,g^{-1}$)	Coulombic efficiency (%)
1st	2186	4676	43.94	1484	1324	112.15
2nd	2151	2354	91.37	1651	1791	92.17
3th	2128	2272	93.65	1670	1726	96.77
10th	1848	1956	94.49	1589	1601	99.21
20th	1486	1559	95.33	1411	1412	99.94
30th	1226	1285	95.47	1106	1116	99.13
40th	1073	1122	95.64	1002	1008	99.31

the CV measurements. In the following half-cycle (Li extraction), two broad peaks appear at around 0.3 and 0.55 V in both electrodes, representing two Li extraction stages, which correspond to silicon, disordered carbon and the CNF.

Fig. 6 shows the voltage profiles of both the original and precharged electrodes in the first cycle with the PEO-based electrolyte. The original electrode had an initial potential of 3.00 V, whereas that of the precharged electrode was 0.41 V. The decrease in potential means that an amount of lithium metal reacts with the compounds and is attributable to the irreversible capacity, as indicated in Fig. 5. Consequently, this improves the coulombic efficiency of the precharged electrode. The discharge capacity of the original electrode was 4976 $mAh\,g^{-1}$, whereas that following the first charge capacity was 2187 $mAh\,g^{-1}$, so that the coulombic efficiency was only 44%. On the other hand, the first discharge capacity of the precharged electrode was only 1324 $mAh\,g^{-1}$ while the charging capacity was 1484 $mAh\,g^{-1}$, which indicates a coulombic efficiency of 112% (the coulombic efficiency of >100% is due to the excess lithium added, because it was difficult to adjust exactly such a small amount of Li metal). Therefore, the lithium sheet functioned well as a reducing agent for the Si/C@CNF electrode during cycling of the battery.

Fig. 7 shows the specific capacities and coulombic efficiencies of the precharged electrode as a function of the cycle number. As shown in Fig. 6, the first discharge and charge capacities of the precharged electrode were 1324 and 1484 $mAh\,g^{-1}$, respectively, of which the values are lower than the returned capacity (2186 $mAh\,g^{-1}$) in the first cycle of the original electrode (Figs. 4b and 6). This may be attributed to the initial inhomogeneous electrode surface caused by attachment of the Li sheet. After several cycles, the capacity in the precharged electrode becomes almost comparable to that in the original electrode (see Table 1). From this point, the lithium metal added has little relation to the reversibility, but is only effective to reduce the first irreversible capacity.

The cycle performance of the original and precharged electrodes is compared in Table 1. After 40 cycles, the capacity of both electrodes is approximately half of the original, which is in contrast to the case of the liquid electrolyte (Fig. 2). This is attributed to many causes; detachment of the particles in the electrode, due to the large volume change of Si during the cycling, the formation of reaction products from decomposition of the polymer contacting the electrode, and the formation of inactive Si–Li alloys by the insertion of a large amount of Li. When the lower cut-off voltage during cycling is less than 0.05 V, it is known that the crystalline $Li_{15}Si_4$ phase appears, from which Li is cannot be easily extracted [18]. However, in the present work, the formation of the crystalline $Li_{15}Si_4$ phase was not observed, but only the amorphous phase remained even with a cut-off voltage of 0.02 V, according to XRD observations. The Si powder used was nanosize silicon (50 nm), and Hatchard and Dahn reported that the crystalline $Li_{15}Si_4$ phase forms only above a critical size of approximately 2 μm [19]. Therefore, the Si used in the present research is considered to be too small to form the crystalline $Li_{15}Si_4$ phase. The capacity fade with cycling may therefore be attributed to imperfections of the electrode texture. Further optimization of the texture and composition of the Si/C@CNF electrode is expected to result in higher performance of the solid polymer lithium battery.

The safety of small-size lithium-ion batteries for conventional applications is well established. In contrast, the safety of large-size lithium-ion batteries is still questionable, especially in the case of abusive use. The safety of lithium-ion batteries is mainly related to the thermal reactivity of the components. Fig. 8 shows differential scanning calorimetry (DSC) curves for three fully lithiated electrodes; (a) the original electrode with the PEO-based electrolyte, (b) the precharged electrode with the PEO electrolyte, and (c) the original electrode with the liquid electrolyte. Only small broad peaks were observed for both the PEO-based electrolyte samples at temperatures higher than 300 °C, while strong peaks appeared for the liquid electrolyte sample from low temperatures of 100 °C. The specific reaction heats for the original and precharged electrodes with the PEO-based electrolyte were 35.7 $J\,g^{-1}$ and 51.2 $J\,g^{-1}$, respectively. The values were normalized on the basis of the heat per discharge capacity to 0.024 $J\,mAh^{-1}$ for the original electrode

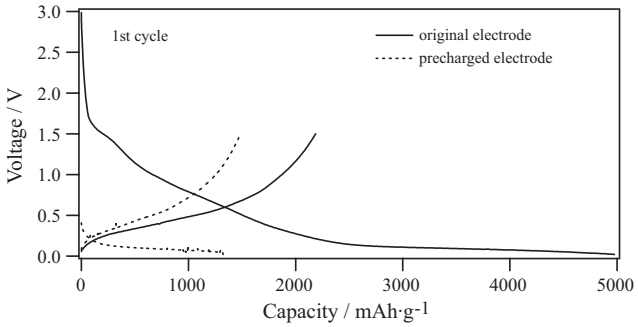

Fig. 6. Charge and discharge curves of the original and precharged electrodes with the PEO-based electrolyte at 60 °C in the first cycle.

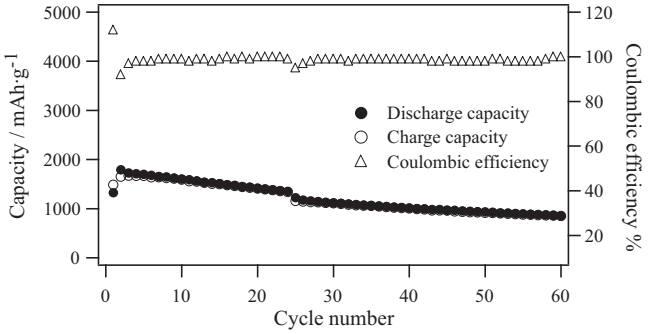

Fig. 7. Cycling performance of the precharged electrode with the PEO-based electrolyte at 60 °C.

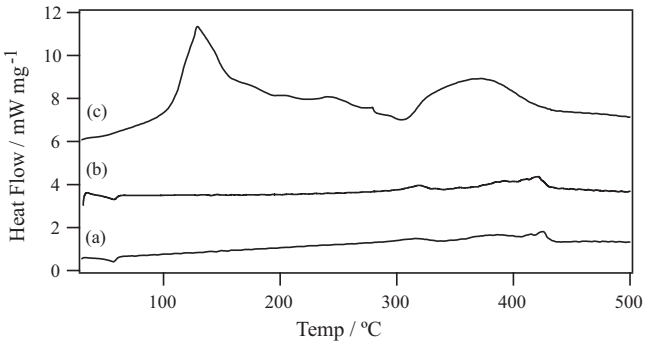

Fig. 8. DSC curves for (a) the original and (b) precharged electrodes with the PEO-based electrolyte and (c) the original electrode with a liquid electrolyte of $LiPF_6$ in EC-DEC.

and 0.034 J mAh^{-1} for the precharged electrode. On the other hand, the specific reaction heat and heat per discharge capacity of the original electrode with the liquid electrolyte were 347.7 J g^{-1} and 0.23 J mAh^{-1}, respectively. This indicates that the solid lithium polymer battery has a large advantage over the liquid electrolyte lithium battery with respect to safety.

4. Conclusions

The lithium insertion and extraction performance of a Si/C@CNF composite electrode for a solid-polymer lithium secondary battery was examined. The electrode showed a high reversible capacity and good cycling performance, although the first cycle irreversible capacity was very high. In order to increase the availability of the Si/C@CNF anode, a "precharged" method using lithium sheet was applied. The coulombic efficiency of the precharged electrode for the first cycle was as high as 112% and after the third cycle, the lithium insertion and extraction efficiency reached almost 100%. A reversible capacity of more than 1000 mAh g^{-1} was maintained after 40 cycles. The Si/C@CNF electrode with the PEO-based electrolyte was revealed to have suitable safety characteristics for practical application. These results should contribute to the development of silicon-based anode materials for solid-polymer lithium-ion batteries.

Acknowledgement

This work was supported by the Cooperation of Innovative Technology and Advanced Research in Evolution Area (City Area) Project of the Ministry of Education, Culture, Sports, Science and Technology of Japan.

References

[1] M. Gauther, D. Fauteux, G. Vassort, A. Belanger, M. Duval, P. Ricoux, J.M. Chabagno, D. Muller, P. Rigaud, M.B. Armand, D. Deroo, J. Electrochem. Soc. 132 (1985) 1333–1340.
[2] C. Brissot, M. Rooso, J.N. Chazalviel, S. Lascaud, J. Power Sources 81–82 (1999) 925–929.
[3] N. Imanishi, Y. Ono, K. Hanai, R. Uchiyama, Y. Liu, A. Hirano, Y. Takeda, O. Yamamoto, J. Power Sources 178 (2008) 744–750.
[4] C.J. Wen, R.A. Huggins, J. Solid State Chem. 37 (1981) 271–278.
[5] C.K. Chan, R. Ruffo, S.S. Hong, R.A. Huggins, Y. Cui, J. Power Sources 189 (2009) 34–39.
[6] B.C. Kim, H. Ueno, T. Satou, T. Fuse, T. Ishihara, M. Ue, M. Senna, J. Electrochem. Soc. 152 (2005) A523–A526.
[7] Q. Si, K. Hanai, N. Imanishi, M. Kubo, A. Hirano, Y. Takeda, O. Yamamoto, J. Power Sources 189 (2009) 761–765.
[8] Y. Liu, K. Hanai, J. Yang, N. Imanishi, A. Hirano, Y. Takeda, Solid State Ionics 168 (2004) 61–68.
[9] P.J. Zuo, G.P. Yin, Z.L. Yang, Z.B. Wang, X.Q. Cheng, D.C. Jia, C.Y. Du, Mater. Chem. Phys. 115 (2009) 757–760.
[10] Y. Liu, J. Yang, N. Imanishi, A. Hirano, Y. Takeda, O. Yamamoto, J. Power Sources 146 (2005) 376–379.
[11] Y. Kobayashi, S. Seki, Y. Mita, Y. Ohno, H. Miyashiro, P. Charest, A. Guerfi, K. Zaghib, J. Power Sources 185 (2008) 542–548.
[12] H.Y. Lee, Y.L. Kim, M.K. Hong, S.M. Lee, J. Power Sources 141 (2005) 159–162.
[13] M.S. Park, S. Rajendran, Y.M. Kang, K.S. Hana, Y.S. Hand, J.Y. Lee, J. Power Sources 158 (2006) 650–653.
[14] T. Li, Y.L. Cao, X.P. Ai, H.X. Yang, J. Power Sources 184 (2008) 473–476.
[15] Q. Si, K. Hanai, T. Ichikawa, A. Hirano, N. Imanishi, Y. Takeda, O. Yamamoto, J. Power Sources 195 (2010) 1720–1725.
[16] D. Saito, Y. Ito, K. Hanai, T. Kobayashi, N. Imanishi, A. Hirano, Y. Takeda, O. Yamamoto, J. Power Sources 195 (2009) 6172–6176.
[17] C.R. Jarvis, M.J. Lain, M.V. Yakovleva, Y. Gao, J. Power Sources 162 (2006) 800–802.
[18] M.N. Obrovac, L. Christensen, Electrochem. Solid State Lett. 7 (2004) A93–A96.
[19] T.D. Hatchard, J.R. Dahn, J. Electrochem. Soc. 151 (2004) A838–A842.